

Highlights

- The reactivity of the molecular anion C_3N^- , proposed to be abundant in Titan's ionosphere, is explored.
- The kinetics and branching ratios of the $C_3^{15}N^- + HC_3^{14}N$ and $C_3^{14}N^- + HC_3^{14}N$ reactions are investigated in the laboratory down to 50 K with the CRESU method.
- Proton transfer is the main exit channel which is indistinguishable with non-isotopically labeled reactants.
- A minor exit channel, reactive detachment, has been uncovered, although the nature of the neutral products has not been identified.
- It is concluded that the $C_3N^- + HC_3N$ reaction cannot contribute to the growth of anions in the upper atmosphere of Titan.

Elusive anion growth in Titan's atmosphere: low temperature kinetics of the $C_3N^- + HC_3N$ reaction

Jérémy Bourgalais^a, Nour Jamal-Eddine^a, Baptiste Joalland^a, Michael Capron^a, Muthiah Balaganesh^a, Jean-Claude Guillemin^b, Sébastien D. Le Picard^a, Alexandre Faure^c, Sophie Carles^a, Ludovic Biennier^{*a}

^a*Institut de Physique de Rennes, Département de Physique Moléculaire, Astrophysique de Laboratoire, UMR CNRS 6251, Université de Rennes 1, Campus de Beaulieu, 35042 Rennes Cedex, France*

^b*Institut des Sciences Chimiques de Rennes, Ecole Nationale Supérieure de Chimie de Rennes, UMR CNRS 6226, 11, Allée de Beaulieu, 35708 Rennes Cedex 7, France*

^c*UJF-Grenoble 1 / CNRS-INSU, Institut de Planétologie et d'Astrophysique de Grenoble (IPAG) UMR 5274, Grenoble, F-38041, France*

Abstract

Ion chemistry appears to be deeply involved in the formation of heavy molecules in the upper atmosphere of Titan. These large species form the seeds of the organic aerosols responsible for the opaque haze surrounding the biggest satellite of Saturn. The chemical pathways involving individual anions remain however mostly unknown. The determination of the rates of the elementary reactions with ions and the identification of the products are essential to the progress in our understanding of Titan's upper atmosphere. We have taken steps in that direction through the investigation of the low temperature reactivity of C_3N^- , which was tentatively identified in the spectra measured by the CAPS-ELS instrument of the Cassini spacecraft during its high altitude flybys. The reaction of this anion with HC_3N , one of the most abundant **trace** organics in the atmosphere, has been studied over the 49–294 K temperature range in uniform supersonic flows using the CRESU technique. The proton transfer is found to be the main exit channel (> 91%) of the $C_3^{15}N^- + HC_3N$ reaction. It remains however indistinguishable with the non-isotopically labeled $C_3^{14}N^-$ reactant. The $T^{-1/2}$ temperature dependence of this proton transfer reaction and its global rate are reasonably well reproduced theoretically using an average dipole orientation model. A minor exit channel, reactive detachment (< 9%), has also been uncovered, although the nature of the neutral products has not been determined. It is concluded that the $C_3^{14}N^- + HC_3N$ reaction cannot contribute to the growth of molecular anions in the upper atmosphere of Titan. Due to the low branching into the neutral exit channel, it cannot contribute either to the growth of neutrals even assuming a complete mass transfer.

Keywords: Titan, atmosphere – Atmospheres, chemistry – Ionospheres

1. Introduction

In a decade of observations, the Cassini **spacecraft** has revolutionized our understanding of Saturn and its surroundings and has lifted the veil over Titan's dense atmosphere and organic-rich

Email address: ludovic.biennier@univ-rennes1.fr (Ludovic Biennier*)

Preprint submitted to ICARUS

chemistry. The atmosphere of the largest moon of Saturn, dominated by nitrogen N_2 (90 – 98%) and methane CH_4 (1 – 6%), contains a wealth of hydrocarbons and nitrogen-bearing molecules. The observed molecular species include acetylene C_2H_2 , polyynes such as diacetylene C_4H_2 , larger hydrocarbons up to benzene C_6H_6 , as well as nitriles such as HCN and HC_3N , with their vertical abundances derived from the analysis of Composite Infrared Spectrometer (CIRS) mid-infrared data (Coustenis et al., 2010) **at the low altitude of 200 km and from Cassini's Ion and Neutral Mass Spectrometer (INMS) between 950 and 1070 km (Waite et al., 2007)**. Despite their low abundance, these trace species play a major role in the production and growth of organic aerosols which form the orange haze that hides the surface of Titan from our eyes. Through their interaction with the incident solar radiation, aerosols have a direct impact on the atmospheric properties, acting in particular as anti-greenhouse agents. The mechanisms of formation and growth of these aerosols remain however elusive.

The upper layer of the atmosphere of Titan is a tumultuous territory where a multitude of photochemical processes occurs. This is attested by the detection of a great variety of chemical species, both neutral and charged. Over targeted flybys, INMS measurements revealed the presence of a large variety of positive ions in the 1–99 amu/q mass range (Waite et al., 2007). Groups of peaks separated by ~ 13 amu were found to coincide with features observed in the neutral spectrum measured with the same instrument. The positive ion spectrum inferred from energy/charge measurements (0–350 amu/q) by the Ion Beam Spectrometer of the Cassini Plasma Spectrometer (CAPS-IBS) showed the existence of heavier ions near 1000 km of altitude. One of the most remarkable **pieces of evidence** of the intense chemical activity in the ionosphere was the discovery of negative ions at altitude of 950–1150 km by the Electron Spectrometer sensor of the Cassini Plasma Spectrometer (CAPS-ELS) (Waite et al., 2007; Coates et al., 2007). Despite the poor resolution of the spectrum ($\Delta m/m \sim 17\%$), three peaks at 22 ± 4 , 44 ± 8 and 82 ± 14 amu/q could be distinguished on the low-mass side and were attributed to CN^- , C_3N^-/C_4H^- and C_5N^- by Vuitton et al. (2009) with the assistance of an ionospheric photochemical model. Further encounters have shown that the highest masses were observed at low flyby altitudes with masses up to 13800 amu/q detected at the altitude of 950 km (Coates, 2009). The highest densities were found at the lowest altitudes of the ionosphere too (Wellbrock et al., 2013). Hence, a clear trend has been extracted from the analysis of the mass spectra, i.e. a shift towards larger masses when the altitude decreases.

The presence of large and abundant charged species in the upper layers of the atmosphere and their apparent growth when the altitude is lowered has stimulated further investigations. Using a model coupling aerosol microphysics and photochemistry, Lavvas et al. (2013) showed that the formation of heavy molecules in the upper atmosphere is directly related to ion processes. In this scenario, macromolecules are formed and grow by ion-neutral reactions in the ionosphere. There they attach efficiently free electrons and recombine with positive ions leading to a rapid gain in mass. As they settle down in the atmosphere, they continue to grow until they reach a size where coagulation takes over. These macromolecules could be key intermediates in the formation of aerosols observed at lower altitude in the stratosphere.

The goal of Lavvas' study was to understand the overall interaction of the aerosols with the ionosphere. The results were obtained assuming an ionosphere with one type of positive ion ($m^+ = 30$ amu/q), one type of negative ion ($m^- = 50$ amu/q), and electrons (Lavvas et al., 2013). It is now necessary to assess the role of the individual ions detected in the ionosphere in order to lead to a better understanding of the aerosol chemical composition in Titan's upper atmosphere. Indeed, the composition of these macromolecules and their formation mechanisms are still largely unknown.

The importance of ion reactions in astronomical objects is well recognized due to the absence of kinetic barriers in many of processes in which they are involved (see e.g. Geppert and Larsson, 2013). The reactivity of positive ions has been extensively studied in the laboratory because of the wide range of applications and the relative ease with which they are produced. With the exception of photo-detachment ($A^- + h\nu \rightarrow A + e^-$) and electron attachment ($A + e^- \rightarrow A^-$) processes, negative ion chemistry represents a more uncharted territory. Although many experimental studies have been conducted to determine the kinetics of anion-neutral reactions (Anicich, 1993; Snow and Bierbaum, 2008), a fraction **of these experiments** has simultaneously led to the determination of the nature of products and even less to the branching ratio of the different exit channels. Complementing kinetics studies, the molecular dynamics of a few anion-neutral reactions has been explored using velocity map imaging (Wester, 2014). In any event, only a few experiments have been performed at temperatures lower than 200 K (Viggiano and Paulson, 1983; Le Garrec et al., 1997; Otto et al., 2008; Biennier et al., 2014) under relevant conditions for chemical models of planetary atmospheres, cometary comae, and interstellar clouds.

Many ion-neutral reactions can be reasonably approximated to point charge systems with their rate constants following the Langevin theory, which is temperature independent. If the polarizability of the ion is high or the polarizability of the neutral is low, the attractive potential between the two polarizable species must be considered (Eichelberger et al., 2003). In the case of polar neutrals, the long-range (anisotropic) charge-dipole interaction term must be added to the ion-induced dipole term in the capture potential energy surface. A negative temperature dependence of the rate coefficients is then observed (Faure et al., 2010).

In an effort to extend our comprehension of low temperature negative ion chemistry, we recently engaged in kinetic studies starting with the reaction of CN^- with cyanoacetylene HC_3N over the 50-300 K temperature range. We found that this reaction leads to the production of C_3N^- with a fast rate that is almost temperature independent (Biennier et al., 2014). In the present work, we extend our investigations to the reaction of C_3N^- with HC_3N . The temperature dependence of the rate constant of this reaction was measured from 294 K down to 49 K using the CRESU technique (French acronym for Cinétique de Réaction en Ecoulement Supersonique Uniforme). Our objective, common to other research groups (see e.g. Zabka et al., 2012, 2014), is to explore the role of reactions involving $C_{2x+1}N^-$ anions in the formation of the heavy ions detected in the upper atmosphere of Titan.

2. Laboratory experiments

The ion chemical reactivity was explored with the CRESU technique over the 49 –294 K temperature range while room temperature measurements were duplicated in a flowing afterglow (FA) reactor.

As the reactants differ by only one proton H^+ , the study was realized with an isotope substituted species in order to discriminate between all possible exit channels.

2.1. Ion-neutral reaction kinetics with a flowing afterglow

The Flowing Afterglow Langmuir Probe – Mass Spectrometer (FALP-MS) apparatus has been described in details elsewhere (Carles et al., 2011). The afterglow is generated by a microwave discharge into a helium buffer gas introduced at a flow rate of ~ 15.7 standard $l \cdot \text{min}^{-1}$ into a continuously pumped chamber. This afterglow initially contains metastable helium atoms He^* and He^+/He_2^+ ions. Argon is introduced downstream at a second entry port at about 1 standard $l \cdot \text{min}^{-1}$ to quench the He^* atoms by Penning ionization ($Ar + He^* \rightarrow Ar^+ + He$). The plasma

is quasi neutral and the electron density ($\sim 10^9 \text{cm}^{-3}$) is adjusted by varying the position of the microwave discharge. The reactor is equipped with a movable quadrupole mass spectrometer and a Langmuir probe to respectively measure the ion population and the electron density along of the reaction zone, which is localized downstream of the flow. The ion precursor is injected upstream the reaction zone. It is converted to **the reactant** anion by dissociative electron attachment (see below). The co-reactant is diluted in helium and the mixture injected through an annular entry port equipped with eight needles via a calibrated flow controller. The rate of disappearance of the ions is measured with varying initial co-reactant densities kept well in excess of the ion density.

2.2. Ion-neutral reaction kinetics with supersonic uniform flows

For temperatures below room temperature, the kinetics of the reaction of $\text{C}_3^{15}\text{N}^-$ with cyanoacetylene, HC_3N , was explored using the CRESU technique (Rowe et al., 1984) under a configuration designed to study anions (Biennier et al., 2014). The main features of the experimental setup, displayed in Fig. 1, are briefly **described** below. A uniform supersonic beam is generated by the isentropic expansion of a buffer gas (He), through a Laval nozzle. Helium is continuously introduced into the reservoir by a calibrated mass flow controller at a typical flow rate of 50–100 standard $\text{l}\cdot\text{min}^{-1}$. Downstream, in the main chamber, the supersonic expansion generated by the nozzle is maintained by a $24000 \text{m}^3\text{hr}^{-1}$ capacity pumping system. The design of the nozzle, as well as the pressures in the reservoir (a few tens of mbar) and in the main chamber (a few tenths of mbar), set the temperature of the supersonic flow. The velocity (several 10^4cm s^{-1}), the density (typically 10^{16} – $10^{17} \text{molecule cm}^{-3}$) and the low temperature of the supersonic flow are kept uniform over several tens of centimeters corresponding to hydrodynamic times of about 100 to 1000 μs . All the other neutral gases necessary for the study of the title reaction are introduced in small amount in the reservoir by means of additional calibrated mass flow controllers. Due to the relatively high density of the flow, frequent collisions occur ensuring thermal equilibrium for all the molecular species present in the supersonic expansion.

The ions are produced in the supersonic flow a few mm downstream of the exit of the nozzle by an electron gun mounted perpendicularly to the molecular beam. The electron beam (12 kV, 200 μA emission current) generates a low density plasma, consisting primarily of buffer gas cations (He^+) and cold ($T_e \sim 500 \text{K}$) secondary electrons ($[\text{e}^-] \sim 4 \times 10^8 - 10^9 \text{cm}^{-3}$).

A unique aspect of this apparatus is its movable quadrupole mass spectrometer (0–200 amu/q), **which measures** the ion signal by skimming out a central portion of the flow at a chosen distance from the tip of the nozzle. A Langmuir probe, which consists of a gold plated tungsten wire of 25 μm diameter and $8.84 \pm 0.05 \text{mm}$ length, is mounted on the skimming cone to probe the electron density in the supersonic flow a few mm ahead the mass spectrometer sampling aperture. **The surface of the Langmuir probe is cleaned before each measurement by electron bombardment, which is activated by polarizing positively the probe.**

2.3. Anion production

One of the challenges of the current experimental configuration lies in the generation of anions in abundance and on a short timescale (a few tens of microseconds) compared to the whole accessible reaction time (between a hundred and a few hundreds of microseconds). To do so, we adopt the same approach employed in our previous experiments (Biennier et al., 2014) based on dissociative electron attachment and consisting in the injection of a molecular precursor in the flow. The precursor must meet the following criteria: (1) it should be sufficiently volatile to be introduced in fair amounts, (2) it must attach cold electrons, and (3) the ion of interest must

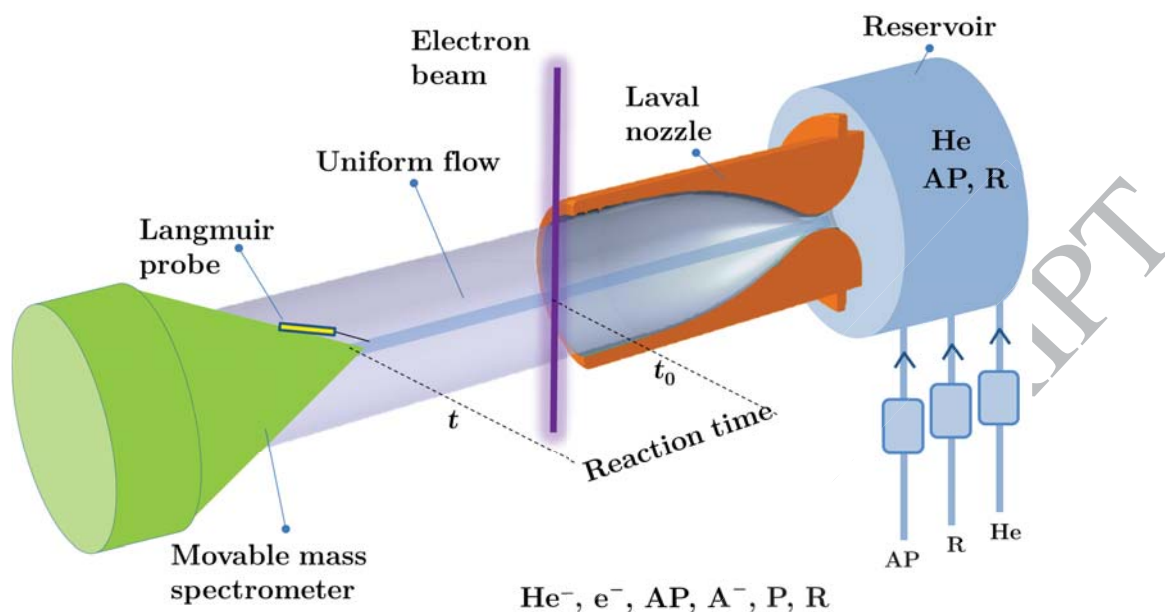


Figure 1: Schematic diagram of the CRESU apparatus showing the retractable Laval nozzle, the ionization region and the moveable quadrupole mass spectrometer/Langmuir probe assembly. AP: anion precursor, R: reactant.

be the dominant product. Bromocyanoacetylene $\text{BrC}_3^{15}\text{N}$ with isotopically labeled nitrogen was selected for that purpose.

The synthesis of bromocyanoacetylene $\text{BrC}_3^{15}\text{N}$ is performed following an approach designed by Kloster-Jensen (1963) for the main isotopologue. In a three necked flask placed in liquid nitrogen, cyanoacetylene HC_3^{15}N (1.2 g) and water (50 ml) are well stirred under an inert atmosphere. A cold potassium bromide/bromine solution (45 ml) is added through a dropping funnel. This solution is prepared in an ice bath by slowly adding bromine (3 ml) to a solution of potassium bromide (7.5 g) in water (50 ml). At the end of the addition of the potassium bromide/bromine solution, a half-normal potassium hydroxide solution (40 ml) is added to the mixture. A fine, heavy precipitate appears. The addition is continued until the precipitation ceases. After that, the mixture is filtered with a Buchner funnel and a white crystalline product is isolated. It is then sublimated in vacuo over phosphorus pentoxide in order to get rid of water. As a result, 1.2 g of bromocyanoacetylene $\text{BrC}_3^{15}\text{N}$ (yield: 40%) is obtained with a purity $\geq 98\%$ on the basis of the ^1H and ^{13}C NMR spectra of a concentrated sample diluted in deuteriochloroform (^{13}C NMR (CDCl_3 , 100 MHz) δ 51.0 ($^2J_{\text{C}_{15}\text{N}} = 8.0 \text{ Hz(d)}$); 55.7 ($^3J_{\text{C}_{15}\text{N}} = 4.4 \text{ Hz(d)}$); 105.1 ($^1J_{\text{C}_{15}\text{N}} = 20.3 \text{ Hz(d)}$)). Bromocyanoacetylene, liquid at room temperature, is finally diluted in helium (at a mole fraction of 0.3%) and injected into the reservoir with a calibrated mass flow controller.

Mass spectrometry measurements performed with the FALP-MS at room temperature revealed that the production of $\text{C}_3^{15}\text{N}^-$ is the main exit channel of the electron dissociative attach-

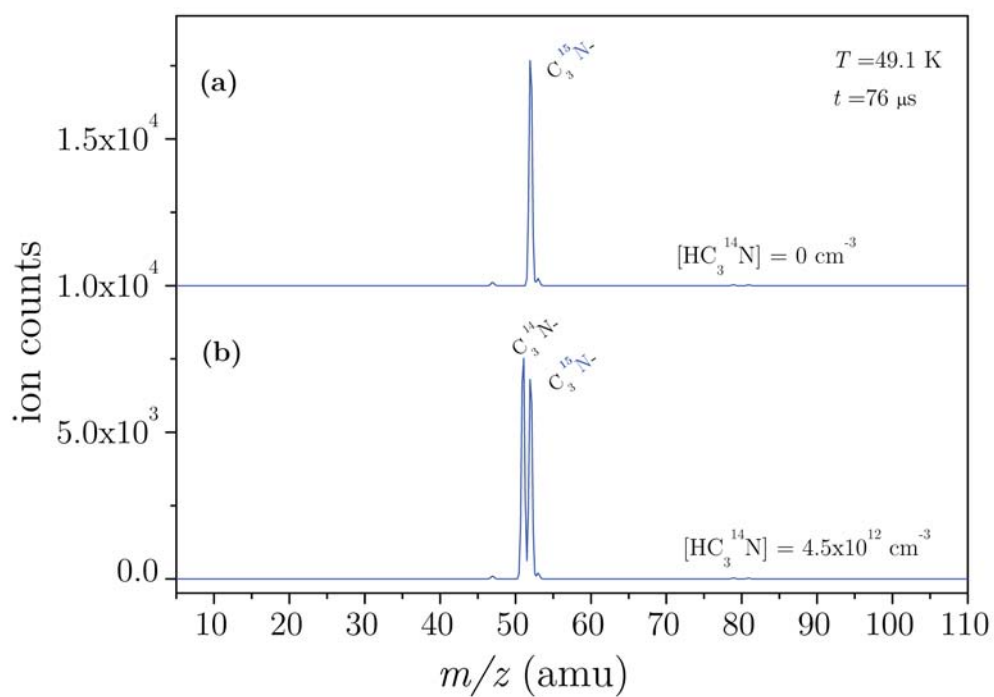
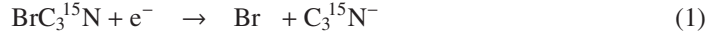


Figure 2: Mass spectroscopic sampling (negative ion mode) of a cold supersonic He flow ($T = 49.1$ K) seeded with small amounts of $BrC_3^{15}N$ and recorded after a reaction time of $t = 76 \mu s$ in absence of co-reactant (a) and in presence of $HC_3^{14}N = 4.5 \times 10^{12} \text{ molecule cm}^{-3}$ (b).

ment reaction (Carles et al., 2015)



This is confirmed by low temperature CRESU measurements as can be seen in Fig. 2 (a) where the two peaks of the stable isotopes of Br^- at $m/z = 79$ and 81 are negligible.

The analysis of the FALP-MS measurements led to the determination of an electron attachment rate for bromoacetylene BrC_3N of $2.04 \times 10^{-7} \text{ cm}^3 \text{ molecule}^{-1} \text{ s}^{-1}$, about two orders of magnitude higher than for cyanogen bromide BrCN (Carles et al., 2015). This means that under similar conditions, the high electron attachment rate will ensure rapid conversion of the precursor into the anion even though the vapor pressure of BrC_3N is much lower than the one of BrCN .

3. Chemical reaction analysis

3.1. Ion time profile

The rate constants of the $\text{C}_3^{15}\text{N}^- + \text{HC}_3\text{N}$ and $\text{C}_3\text{N}^- + \text{HC}_3\text{N}$ reactions are determined by numerically integrating a system of five coupled differential equations which describe the time evolution of all charged species, the precursor and the reactant in excess:

$$\begin{aligned} \frac{d\text{C}_3^{15}\text{N}^-}{dt} &= +k_2[\text{BrC}_3^{15}\text{N}][\text{e}^-] & (2) \\ &\quad -k_{15}[\text{HC}_3\text{N}]\text{C}_3^{15}\text{N}^- - D_1\text{C}_3^{15}\text{N}^- \\ \frac{d[\text{BrC}_3^{15}\text{N}]}{dt} &= -k_2[\text{BrC}_3^{15}\text{N}][\text{e}^-] \\ \frac{d[\text{e}^-]}{dt} &= -k_2[\text{BrC}_3^{15}\text{N}][\text{e}^-] \\ \frac{d[\text{HC}_3\text{N}]}{dt} &= -k_{15}[\text{HC}_3\text{N}]\text{C}_3^{15}\text{N}^- - k_{14}[\text{HC}_3\text{N}]\text{C}_3\text{N}^- \\ \frac{d\text{C}_3\text{N}^-}{dt} &= +k_{15}[\text{HC}_3\text{N}]\text{C}_3^{15}\text{N}^- - D_2\text{C}_3\text{N}^- \\ &\quad -k_{14}[\text{HC}_3\text{N}]\text{C}_3\text{N}^- \end{aligned}$$

with $\text{C}_3^{15}\text{N}^-$ and C_3N^- the scaled ion signals, $[\text{BrC}_3^{15}\text{N}]$, $[\text{HC}_3\text{N}]$, and $[\text{e}^-]$ the bromoacetylene, cyanoacetylene and electron densities in the supersonic uniform beam in cm^{-3} , k_{15} the global reaction rate of the reaction $\text{C}_3^{15}\text{N}^- + \text{HC}_3\text{N}$, k_2 the dissociative attachment rate, k_{14} the global rate of the $\text{C}_3\text{N}^- + \text{HC}_3\text{N}$ reaction, D_1 and D_2 the first order rates coefficient taking into account molecular diffusion and reactions of the ions with impurities.

The reaction starting time, t_0 , which is defined by the intersection of the electron beam with the supersonic flow, is treated as a free adjustable parameter for each temperature. The shortest reaction times, below a few tens of microseconds (meaning short distances between the tip of the mass spectrometer and the electron beam) are not accessible experimentally. The densities of $[\text{BrC}_3^{15}\text{N}]$, $[\text{HC}_3\text{N}]$ and $[\text{e}^-]$ at t_0 are accurately known for each temperature and constitute the initial parameters of the differential equation system. For each ion, the signal is set to zero at the integration starting time. The $[\text{BrC}_3^{15}\text{N}]$ density is assumed to be constant throughout the entire dataset for all temperatures and for given values of the HC_3N density. Molecular diffusion

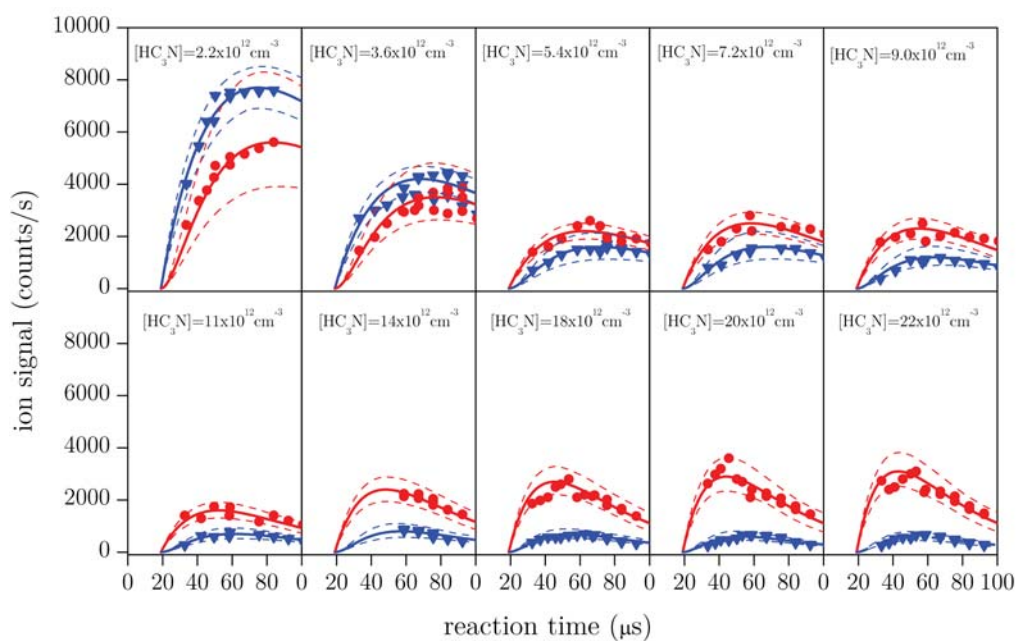


Figure 3: Time evolution of $C_3^{15}N^-$ (\blacktriangledown) and $C_3^{14}N^-$ (\bullet) ion populations (in $\text{counts}\cdot\text{s}^{-1}$) at $T = 157.5$ K in presence of various initial $[HC_3N]$ number densities, best fit values (full lines).

plays a significant role only for room temperature experiments (Biennier et al., 2014). For each temperature, the algorithm optimizes a modified version of χ^2 . This function represents the difference between the experimental and calculated data and takes into account the full set of data (all [HC₃N] densities) at a given temperature.

$$\chi^2(T) = \frac{1}{n} \sum_{i=1}^n \frac{1}{m_i} \sum_{j=1}^{m_i} \left\{ \left(C_3^{15}N_{\text{exp}}^-(t_j) - C_3^{15}N_{\text{calc}}^-(t_j) \right)^2 + \left(C_3N_{\text{exp}}^-(t_j) - C_3N_{\text{calc}}^-(t_j) \right)^2 \right\} \quad (3)$$

with n the number of different [HC₃N] densities and m_i the number of measurements of the two anions for the i th value of [HC₃N].

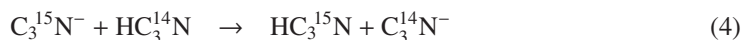
To minimize χ^2 , we select a Nelder-Mead simplex algorithm used to find the minimum of unconstrained multi-variable function using derivative-free method starting with an initial estimate (Nelder and Mead, 1965). This algorithm converges reasonably quickly under our conditions and has the advantage of being very robust (Lagarias et al., 1998). In order to estimate the uncertainty associated with the results, we perform Monte-Carlo simulations in which several surrogate datasets are generated in order to mimic experimental errors (determination of the mass peak maxima at fast mass scanning rates) and/or fluctuations (mass flows, pressures, ...). The derived rate constants and their associated errors are given in Table 1.

Table 1: Rate coefficients **and branching ratios** for the reactions of $C_3^{15}N^-$ and $C_3^{14}N^-$ with cyanoacetylene, HC₃N over the 49–294 K temperature range.

T	k_{15}	exit channels		k_{14}	exit channel	n_{tot}	[HC ₃ N]	Method
K	$\times 10^{-9}$	H ⁺ exch.	RD	$\times 10^{-9}$	RD	$\times 10^{16}$	$\times 10^{12}$	
	cm ³ molec. ⁻¹ s ⁻¹			cm ³ molec. ⁻¹ s ⁻¹		cm ⁻³	cm ⁻³	
49.1	6.1 ± 1.5	0.91	0.09	0.54 ± 0.13	1	10.4	3.1–25	CRESU
71.6	5.7 ± 2.3	0.94	0.06	0.36 ± 0.11	1	6.01	1.2–11	CRESU
157.5	2.4 ± 0.5	0.91	0.09	0.22 ± 0.04	1	13.0	2.2–22	CRESU
294	2.0 ± 0.6	0.91	0.09	0.18 ± 0.05	1	7.47	3.2–51.8	CRESU
294	1.98 ± 0.12	0.91	0.09	0.17 ± 0.04	1	1.74	0.44–15.2	FALP

3.2. Reaction products and mechanisms

Mass spectra show that, as soon $C_3^{15}N^-$ is generated by dissociative electron attachment, it reacts with HC₃¹⁴N by proton exchange (see Fig. 2 (b)):



To gain insight into the energetics of this reaction, quantum chemistry calculations at the CBS-QB3 level of theory are performed. CBS-QB3 is a composite *ab initio* method that involves geometry optimization and evaluation of vibrational frequencies at the B3LYP/6-311(2d,d,p)

level of theory and a series of Coupled-Cluster and Møller-Plesset single-point calculations with various basis sets in order to extrapolate to the complete basis set limit (Montgomery et al., 2000). The reactants first produce a complex of linear structure $\text{NCCC}^- \cdots \text{HCCCN}$. This barrierless process is estimated to be ~ 77.4 kJ/mol exoergic after correction for zero-point vibrational energies. To migrate, the proton must overcome a transition state located at 10.0 kJ/mol above this deep well.

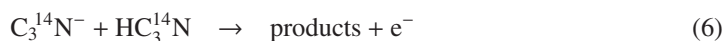
On the basis of these theoretical results, we expect the proton transfer to occur rapidly because its corresponding barrier is low compared to the significant internal energy of the complex. This is confirmed by the fact that the complex at $m/z = 102$ is not detected. No product ion **other than** $\text{C}_3^{14}\text{N}^-$ is detected. In particular, the $m/z = 75$ $\text{C}_5^{15}\text{N}^-$ ion is absent in the mass spectra, although the $\text{C}_5\text{N}^- + \text{HCN}$ exit channel has been observed in tandem mass spectrometry experiments by Zabka et al. (2014). According to their *ab initio* calculations, there is an exothermic pathway leading to the formation of these products ($\Delta_r H(0\text{K}) = -36$ kJ mol $^{-1}$), which involves a series of rearrangements of the complex including several transition states located near the dissociation limit. However, we show here that one single collision between HC_3N and C_3N^- does not permit the reactive system to follow this pathway. Larger anionic complexes with several units of HC_3N must therefore be involved in the formation process of C_5N^- , as suggested by Zabka et al. (2014).

Interestingly, mass spectra show that the secondary ion $\text{C}_3^{14}\text{N}^-$ ($m/z = 50$) reacts with HC_3N , although no ion product is detected for this process. This cannot be explained by proton transfer which is not observable here as the reactants and products are indistinguishable. Both CRESU and FALP measurements indicate that the loss of $\text{C}_3^{14}\text{N}^-$ depends on the HC_3N density. This is even striking in the latter case as the production of the primary ion is completed well before the injection of the co-reactant. This excludes molecular diffusion and reactions with impurities contained in the buffer gas that are independent of $[\text{HC}_3\text{N}]$. Mutual anion-cation neutralization of C_3N^- with positive daughter ions of HC_3N , a process which would depend on cyanoacetylene density, can also be ruled out because positive ion counts remain low. This would indeed translate into an unrealistically high recombination rate well in excess of 10^{-6} cm 3 molecule $^{-1}$ s $^{-1}$. Mutual neutralization (MN) rate constants for molecules containing more than 2 atoms appear reasonably represented by a simple relationship, regardless of the nature of the reacting species:

$$k_{\text{MN}} = (2.8 \pm 1.0) \times 10^{-7} \left(\frac{T}{300 \text{ K}} \right)^{-0.9 \pm 0.1} (m_r)^{-0.5 \pm 0.1} \times (E_a)^{-0.13 \pm 0.04} \text{ cm}^3 \text{ molecule}^{-1} \text{ s}^{-1} \quad (5)$$

with E_a (eV) the binding energy of the electron in the anion (4.305 eV for C_3N^- (Yen et al., 2009)), and m_r (amu) the reduced mass. MN rates can reach values slightly higher than 10^{-7} cm 3 molecule $^{-1}$ s $^{-1}$ at room temperature and for light species, but this is clearly insufficient to explain the depletion of $\text{C}_3^{14}\text{N}^-$ ions we observe.

As a matter of fact, the observations and the above arguments support a reactive detachment (RD) process:



The rate coefficient for RD that we measure here is of the same order of magnitude as previous studies (see e.g. Viggiano et al. (1990)), further supporting this scenario. Unfortunately, we were not able to identify the neutral products of this reaction. The branching ratio associated with this channel, given by the k_{14}/k_{15} ratio, is 9–6%, while it is 91–94% for proton exchange ($[k_{15} - k_{14}]/k_{15}$). The branching ratios appear constant over the temperature range considered.

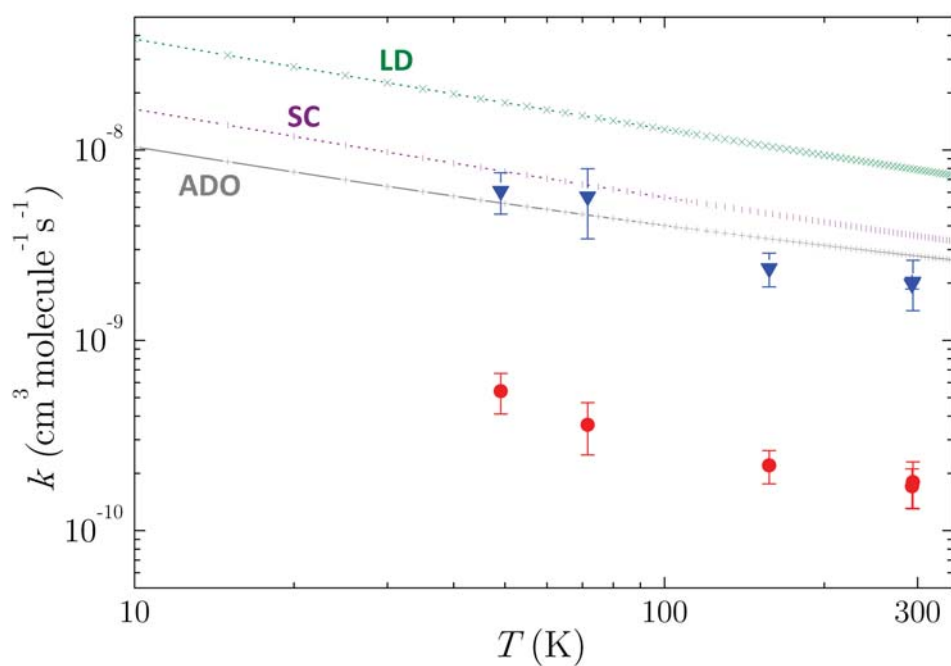


Figure 4: Global rate coefficients for the reactions of $C_3^{15}N^- + HC_3^{14}N$ (▼) and $C_3^{14}N^- + HC_3^{14}N$ (●) over the 49–294 K temperature range. LD: Locked Dipole model; SC: Su & Chesnavich model; ADO: Average Dipole Orientation model.

3.3. Temperature dependence

The $C_3^{15}N^- + HC_3N$ reaction rate shows a negative temperature dependence over the 49-294 K range (Fig. 4). Over this temperature range, the rate coefficient is multiplied by a factor of 3. The Langevin rate, arising from ion-induced dipole interactions, is estimated to $k_L = 1.07 \times 10^{-9} \text{ cm}^3 \text{ molecule}^{-1} \text{ s}^{-1}$ which is smaller by a factor of 6 than the experimental value at 49.1 K. It is undeniable that ion-dipole interactions play a non-negligible role in this reaction, especially at low temperatures. Considering the polarizability $\alpha = 5.24 \times 10^{-24} \text{ cm}^3$ (Baranov and Bohme, 2001) and the dipole moment¹ $\mu = 3.724$ Debye of HC_3N , the rate coefficients corresponding to the locked dipole model, are calculated with the formula (SI units):

$$k_{LD} = \frac{2\pi q}{(4\pi\epsilon_0 m_r)^{1/2}} \left[\alpha^{1/2} + \mu \left(\frac{2}{4\pi\epsilon_0 \pi k_B T} \right)^{1/2} \right] \quad (7)$$

where q is the elementary charge, ϵ_0 is the vacuum permittivity, k_B is the Boltzmann constant. In this model, the rotation is considered as frozen and the dipole orientation is locked toward the ion direction. Then, this ideal situation corresponds to an asymptotical upper limit value when the temperature reaches zero with a temperature dependence in $T^{-1/2}$. The Locked Dipole rate coefficients k_{LD} shown in the Figure 4, are indeed systematically higher than the experimental values over the whole temperature range. The Chesnavich et al. (1980) model, based on the variational rate theory, gives a rate coefficient equals to $k_{SC} = k_L \times k_{cap}$. For the studied reaction, k_{cap} can be written as:

$$k_{cap} = 0.4757 \left[\frac{\mu}{(4\pi\epsilon_0 2\alpha k_B T)^{1/2}} \right] + 0.6200 \quad (8)$$

Overall, the Su & Chesnavich model is in good agreement with the experimental data although it slightly overestimates the rate coefficients for the highest temperatures. The rate coefficients can be alternatively reproduced by the Average Dipole Orientation (ADO) model which corresponds to a correction of the second term in the k_{LD} expression. This correction is a multiplying factor $C = 0.25$ deduced from a polynomial fit extrapolating several experimental dipole moment / polarizability ratios (Su and Bowers, 1973a,b). In this case, the agreement is good for the whole temperature range. We note that this model with $C = 0.25$ corresponds exactly to the infinite-order-sudden (IOS) approximation, which assumes that the ion-dipole interaction is simply averaged over the orientation angles of the colliding partners (see the discussion in Biennier et al. 2014).

The electron detachment rate coefficient exhibits also a negative temperature dependence, which follows a $T^{-0.60}$ power law. This dependence agrees well with the measurements by Viggiano and Paulson (1983) over the 88-468 K for the detachment reactions of $O^- + NO$, $S^- + CO$ and $S^- + O_2$.

4. Implications for the growth of anions in Titan's ionosphere

Lavvas et al. (2013) recently provided a self consistent picture for the growth of heavy molecules from fifty to **thousands of amu** in the upper atmosphere of Titan, thus highlighting the contribution of ion chemistry. The role of the individual ions remains however to be

¹Handbook of Chemistry & Physics 74th Edition, edited by Lide, D. R. (1994)

investigated. Valuable guidelines on the nature of the individual ions can be found in the only photochemical model of Titan's upper atmosphere dedicated to negative ions, which was elaborated by Vuitton et al. (2009). The fact that the model falls short of explaining the CAPS-ELS negative ion observations by one order of magnitude is not prohibitive. There are several potential sources of discrepancies between the model and the observations. They first include the ion count calibration of the instrument which was not intended to measure negative ions. Secondly some chemical pathways may be missing or incorrectly taken into account in terms of product exit channels or rate coefficients because of incomplete or absent laboratory data. Thirdly, the model rests on a bottom-up approach in which molecular species are synthesized step by step. Top-down generation of ions through e.g. dissociative electron attachment of heavy ions is simply not taken into account. Despite these shortcomings, this model seems reasonable and the chemical arguments sound, it represents therefore the best option to follow.

Vuitton's model draws our attention on two negative ions in high abundance ($> 0.1 \text{ cm}^{-3}$) at 1000 km: CN^- and C_3N^- . These anions are thought to play a key role in the growth of heavier species, which are also plentiful. The smallest ion, CN^- is assumed to be generated mainly by hot electron attachment on HCN and HC_3N , with respective abundances inferred from the INMS data of 190 and 34 ppm at 1015 km (Vuitton et al., 2009). At altitudes below 800 km, the reaction of C_xH^- with HCN is supposed to contribute at the same level to the generation of this small anion. The production of the second member of the family, C_3N^- , is mainly achieved at high altitudes through two processes. The first one is the ion-molecule reaction:



which is fast as confirmed by low temperature experiments (Biennier et al., 2014). The second pathway is radiative electron attachment:



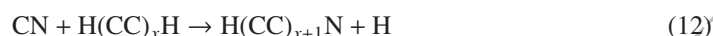
At altitudes lower than 850 km, the reaction:



is expected to contribute significantly to the production of C_3N^- as well (Vuitton et al., 2009). Although many uncertainties persist on the nature of the products and the rates of the last two formation exit channels, even less is known on the loss mechanisms of C_3N^- and their efficiency.

These considerations motivated the current work in its effort to explore the ion growth chemical routes involving C_3N^- . Cyanoacetylene HC_3N appeared as an efficient reactive partner for that purpose for two main reasons. First theoretical calculations showed that the $\text{C}_3\text{N}^- + \text{HCN}$ exit channel was slightly exothermic (Zabka et al., 2012). Second, cyanoacetylene is one of the most abundant polar species in Titan's atmosphere, after hydrogen cyanide HCN. Because of the polar nature of HC_3N , the rate coefficient was then expected to be fast as it depends strongly on the dipole moment μ . Because of the possible existence of an ion product channel, the reaction was expected to be of significance for the early phase of the anion growth sequence. Contrasting with these hypotheses, our experimental results demonstrate that under Titan's low temperature conditions the reaction of C_3N^- with HC_3N does not produce anions. To the contrary, the reactive collision leads to the loss of the electron. Even if polyatomic neutrals with low frequency modes are the most efficient detachers (such as cyanoacetylene), this route remains slow compared to e.g. charge transfer reactions.

In addition, the minor reactive detachment channel cannot contribute significantly to the growth of neutrals, even assuming a mass gain. To prove that point, we compare sections of the neutral and ion chemical networks focusing on the reactivity of the CN and C₃N radicals whose abundances in the ionosphere are around 10 ppb at 1000 km (Vuitton et al., 2009). Recent kinetic studies showed that the C₃N radical was highly reactive down to low temperatures (Fournier, 2014). The aim of that work was to investigate the propagation/cyanopolyynes conversion as a source of long chains with C₃N similarly to what was proposed for the CN radical:



To achieve this goal, Fournier (2014) studied the reaction of C₃N with the hydrocarbons C₂H₂, C₂H₄, C₂H₆, C₃H₄, C₃H₆ and C₃H₈ with the CRESU over the 24–294 K temperature domain, and measured fast rates in the $2\text{--}6 \times 10^{-10} \text{ cm}^3 \text{ molecule}^{-1} \text{ s}^{-1}$ range. These results indicate that the C₃N radical could represent a key species **in the growth** of larger cyanopolyynes H(C≡C)_xCN. The same study has not been conducted so far for the reaction of C₃N + HC₃N. However, some insights can be gained from the investigation of the CN + HC₃N reaction with the CRESU over the 22–294 K temperature range performed by Cheikh Sid Ely et al. (2013). We justify this approach because in the case of reactions with hydrocarbons, the rates with the CN radical have been found always close or slightly lower than with C₃N (Sims et al., 1993; Carty et al., 2001; Morales et al., 2010). This suggests that CN and C₃N radicals could follow a similar chemical behavior with cyanopolyynes. The idea is to derive a lower limit for the rate coefficient. The derived rate coefficient of the CN + HC₃N reaction depends markedly on the temperature, gaining one order of magnitude when going from 294 K to 22 K. At an altitude of 1000 km, characterized by a typical temperature of 170 K, this translates into a rate of $2.6 \times 10^{-11} \text{ cm}^3 \text{ molecule}^{-1} \text{ s}^{-1}$. There is only one exothermic bimolecular channel for this reaction leading to C₄N₂ + H. In absence of further data, we adopt the same rate for the C₃N + HC₃N reaction, which is one order of magnitude lower than the rate of the reactive detachment channel. According to theoretical calculations of end-products for the C₃N + HC₃N reaction, there are two exothermic bimolecular exit channels which are CN + HC₅N ($\Delta_r H(0 \text{ K}) = -60.1 \text{ kJ mol}^{-1}$) and NC₆N + H ($\Delta_r H(0 \text{ K}) = -133.9 \text{ kJ mol}^{-1}$) (values calculated at the CBS-QB3 level of theory). The branching into the different exothermic channels will be controlled by the presence of transition states but anyhow all routes lead to a mass gain. If we now adopt the C₃N⁻/C₃N ratio of 1.9×10^{-3} in the ionosphere proposed by Vuitton et al. (2009), we calculate that the reactive detachment route contributes at most to 1.5% to the production of neutrals considering only the equivalent radical-neutral reaction. This small value demonstrates that the C₃N⁻ + HC₃N reaction is not significant for neutral growth either.

The family of C_{2x+1}N molecular species displays a high electron affinity. As a consequence, these species will not easily give away their electrons, and their negative counterparts may rather constitute end-products than intermediates in heavy ions production. **An alternative is to investigate** the reactivity of C_x⁻ and C_xH⁻ ions to explore ion growth. Some insights may be gained from astronomical observations of interstellar ions. Three members of the C_xH⁻ ions have been individually identified in the interstellar medium (Thaddeus et al., 2008; Cernicharo et al., 2008; Agundez et al., 2010). **Pure carbon chains are also expected to be present, but since they lack a permanent dipole moment, they escape detection with radio-telescopes.**

5. Conclusions

One of the key questions that has been addressed here is the formation kinetics and mechanisms of one of the smallest negative ions detected in Titan's ionosphere. This is of interest because the anions **are presumed to trigger** the production of the heavier species that will form the seeds of the organic aerosols responsible for the opaque haze. With this aim in mind, we have measured the kinetics of the reaction of C_3N^- with cyanoacetylene over the 49-294 K temperature range. We have found that proton transfer is the main exit channel (> 91%), which is indistinguishable with non-isotopically labeled reactants. The $T^{-1/2}$ temperature dependence of this reaction and its global rate are reasonably well reproduced by the average dipole orientation model. A minor exit channel, reactive detachment (< 9%), has also been uncovered, although the nature of the neutral products of this second exit channel has not been identified yet. We conclude that the $C_3N^- + HC_3N$ reaction cannot contribute to the growth of molecular anions in the upper atmosphere of Titan. The formation mechanism of C_5N^- , which has been proposed by Vuitton et al. (2009) to account for the peak around m/z 74, remains elusive. Supposing that the minor neutral channel was leading to some mass transfer, its low branching ratio excludes any significant contribution to the growth of neutrals.

6. Acknowledgments

This research was supported by the French National Research Agency (ANR) through a grant to the Anion Cos Chem project (ANR-14-CE33-0013), the CNRS-INSU Programme National de Physique et Chimie du Milieu Interstellaire and the CNRS-INSU Programme National de Planétologie. We thank Daniel Cordier for his help concerning the kinetics analysis. This work also benefited from discussions with our colleagues Ján Žabka, Christian Alcaraz, Claire Romanzin, Véronique Vuitton and Roland Thissen. J.-C. G. thanks the Centre National d'Etudes Spatiales (CNES) for financial support. S. L. P. thanks the Institut Universitaire de France (IUF) for financial support.

References

- Agundez, M., Cernicharo, J., Gulin, M., Kahane, C., Roueff, E., Klos, J., Aoiz, F. J., Lique, F., Marcelino, N., Goicoechea, J. R., Gonzalez Garcia, M., Gottlieb, C. A., McCarthy, M. C., Thaddeus, P., 2010. Astronomical identification of CN^- , the smallest observed molecular anion. *Astronomy & Astrophysics* 517, L2.
- Anicich, V. G., 1993. Evaluated Bimolecular Ion-Molecule Gas Phase Kinetics of Positive Ions for Use in Modeling Planetary Atmospheres, Cometary Comae, and Interstellar Clouds. *Journal of Physical and Chemical Reference Data* 22 (6), 1469–1569.
- Baranov, V., Bohme, D. K., 2001. Coordination chemistry of Fe^+ , $(c-C_5H_5)Fe^+$, and $(c-C_5H_5)_2Fe^+$ in the gas phase at room temperature: kinetics of sequential ligation with hydrogen cyanide and cyanoacetylene. *International Journal of Mass Spectrometry* 210-211, 303–310.
- Biennier, L., Carles, S., Cordier, D., Guillemin, J.-C., Le Picard, S. D., Faure, A., 2014. Low temperature reaction kinetics of $CN^- + HC_3N$ and implications for the growth of anions in Titan's atmosphere. *Icarus* 227, 123–131.
- Carles, S., Adjali, F., Monnerie, C., Guillemin, J. C., Le Garrec, J. L., 2011. Kinetic studies at room temperature of the cyanide anion CN^- with cyanoacetylene (HC_3N) reaction. *Icarus* 211 (1), 901–905.
- Carles, S., Le Garrec, J.-L., Guillemin, J.-C., Biennier, L., 2015. Chemistry of Nitrile Anions in the Interstellar Medium. *AIP Conference Proceedings*.
- Carty, D., Le Page, V., Sims, I. R., Smith, I. W. M., 2001. Low temperature rate coefficients for the reactions of CN and C_2H radicals with allene ($CH_2=C=CH_2$) and methyl acetylene (CH_3CCH). *Chemical Physics Letters* 344, 310–316.
- Cernicharo, J., Guélin, M., Agundez, M., McCarthy, M. C., Thaddeus, P., 2008. Detection of C_5N^- and Vibrationally Excited C_6H in IRC +10216. *The Astrophysical Journal Letters* 688 (2), L83.

- Cheikh Sid Ely, S., Morales, S., Guillemin, J.-C., Klippenstein, S. J., Sims, I., 2013. Low Temperature Rate Coefficients for the Reaction $CN + HC_3N$. *Journal of Physical Chemistry A* 117, 12155–12164.
- Chesnavich, W. J., Su, T., Bowers, M. T., 1980. Collisions in a noncentral field: A variational and trajectory investigation of ion-dipole capture. *J Chem Phys* 72 (4), 2641–2655.
- Coates, A. J., 2009. Interaction of Titan's ionosphere with Saturn's magnetosphere. Vol. 367.
- Coates, A. J., Crary, F. J., Lewis, G. R., Young, D. T., Waite, J. H., J., Sittler, E. C., J., 2007. Discovery of heavy negative ions in Titan's ionosphere. *Geophysical Research Letters* 34 (22), L22103.
- Coustonis, A., Jennings, D. E., Nixon, C. A., Achterberg, R. K., Lavvas, P., Vinatier, S., Teanby, N. A., Bjoraker, G. L., Carlson, R. C., Piani, L., Bampasidis, G., Flasar, F. M., Romani, P. N., 2010. Titan trace gaseous composition from CIRS at the end of the Cassini-Huygens prime mission. *Icarus* 207, 461–476.
- Eichelberger, B. R., Snow, T. P., Bierbaum, V. M., 2003. Collision rate constants for polarizable ions. *Journal of the American Society for Mass Spectrometry* 14 (5), 501–505.
- Faure, A., Vuitton, V., Thissen, R., Wiesenfeld, L., Dutuit, O., 2010. Fast ion-molecule reactions in planetary atmospheres: a semiempirical capture approach. *Faraday Discussions* 147, 337.
- Fournier, M., 2014. Reactivity of C_3N and C_2H at low temperature: applications for the Interstellar Medium and Titan. Ph.D. thesis.
- Geppert, W. D., Larsson, M., 2013. Experimental investigations into astrophysically relevant ionic reactions. *Chem Rev* 113 (12), 8872–8905.
- Kloster-Jensen, E., 1963. Unsaturated Hydrogen-Free Halogeno Cyano Compounds. II. Synthesis and general properties of bromocynoacetylene. *Acta Chem. Scand.* 17, 1862–1865.
- Lagarias, J. C., Reeds, J. A., Wright, M. H., Wright, P. E., 1998. Convergence properties of the nelder-mead simplex method in low dimensions. *SIAM Journal on optimization* 9 (1), 112–147.
- Lavvas, P., Yelle, R. V., Koskinen, T., Bazin, A., Vuitton, V., Vigren, E., Galand, M., Wellbrock, A., Coates, A. J., Wahlund, J.-E., Crary, F. J., Snowden, D., 2013. Aerosol growth in Titan's ionosphere. *Proceedings of the National Academy of Sciences* 110, 2729–2734.
- Le Garrec, J.-L., Rowe, B. R., Queffelec, J. L., Mitchell, J. B. A., Clary, D. C., 1997. Temperature dependence of the rate constant for the $Cl^- + CH_3Br$ reaction down to 23 K. *J Chem Phys* 107 (3), 1021–1024.
- Montgomery, J. A., Frisch, M. J., Ochterski, J. W., Petersson, G. A., 2000. A complete basis set model chemistry. VII. Use of the minimum population localization method. *J Chem Phys* 112, 6532.
- Morales, S. B., Le Picard, S. D., Canosa, A., Sims, I. R., 2010. Experimental measurements of low temperature rate coefficients for neutral-neutral reactions of interest for atmospheric chemistry of Titan, Pluto and Triton: Reactions of the CN radical. *Faraday Discussions* 147, 155.
- Nelder, J. A., Mead, R., 1965. A simplex method for function minimization. *The computer journal* 7 (4), 308–313.
- Otto, R., Mikosch, J., Trippel, S., Weidemüller, M., Wester, R., 2008. Nonstandard behavior of a negative ion reaction at very low temperatures. *Phys Rev Lett* 101 (6), 063201.
- Rowe, B. R., Dupeyrat, G., Marquette, J. B., Gaucherel, P., 1984. Study of the reactions $N_2^+ + 2N_2 \rightarrow N_4^+ + N_2$ and $O_2^+ + 2O_2 \rightarrow O_3^+ + O_2$ from 20 to 160 K by the CRESU technique. *J. Chem Phys.* 80 (10), 4915–4921.
- Sims, I. R., Queffelec, J.-L., Travers, D., Rowe, B. R., Herbert, L. B., Karthuser, J., Smith, I. W. M., 1993. Rate constants for the reactions of CN with hydrocarbons at low and ultra-low temperatures. *Chemical Physics Letters* 211, 461–468.
- Snow, T. P., Bierbaum, V. M., 2008. Ion chemistry in the interstellar medium. *Annual Review of Analytical Chemistry* 1, 229–259.
- Su, T., Bowers, M. T., 1973a. Ion-Polar molecule collisions: the effect of ion size on ion-polar molecule rate constants; the parameterization of the average-dipole-orientation theory. *International Journal of Mass Spectrometry and Ion Physics* 12 (4), 347–356.
- Su, T., Bowers, M. T., 1973b. Theory of ionpolar molecule collisions. Comparison with experimental charge transfer reactions of rare gas ions to geometric isomers of difluorobenzene and dichloroethylene. *J Chem Phys* 58 (7), 3027–3037.
- Thaddeus, P., Gottlieb, C. A., Gupta, H., Bruenken, S., McCarthy, M. C., Agundez, M., Guelin, M., Cernicharo, J., 2008. Laboratory and astronomical detection of the negative molecular ion C_3N^- . *Astrophysical Journal* 677 (2), 1132–1139.
- Viggiano, A. A., Morris, R. A., Paulson, J. F., 1990. Kinetic energy and temperature dependences of the rate constants for electron detachment of oxonitrate(1-) by nitrogen oxide (N_2O), carbon dioxide, nitrogen, methane, ethane, and propane. *Journal of Physical Chemistry* 94 (8), 3286–3290.
- Viggiano, A. A., Paulson, J. F., 1983. Temperature dependence of associative detachment reactions. *J Chem Phys* 79 (5), 2241–2245.
- Vuitton, V., Lavvas, P., Yelle, R. V., Galand, M., Wellbrock, A., Lewis, G. R., Coates, A. J., Wahlund, J. E., 2009. Negative ion chemistry in Titan's upper atmosphere. *Planetary and Space Science* 57 (13), 1558–1572.
- Waite, J. H., Young, D. T., Cravens, T. E., Coates, A. J., Crary, F. J., Magee, B., Westlake, J., 2007. The Process of Tholin Formation in Titan's Upper Atmosphere. *Science* 316 (5826), 870–875.

- Wellbrock, A., Coates, A. J., Jones, G. H., Lewis, G. R., Waite, J. H., 2013. Cassini CAPS-ELS observations of negative ions in Titan's ionosphere: Trends of density with altitude. *Geophysical Research Letters* 40 (17), 4481–4485.
- Wester, R., 2014. Velocity map imaging of ion-molecule reactions. *Physical Chemistry Chemical Physics* 16 (2), 396–405.
- Yen, T. A., Garand, E., Shreve, A. T., Neumark, D. M., 2009. Anion Photoelectron Spectroscopy of C_3N^- and C_5N^- . *The Journal of Physical Chemistry A* 114 (9), 3215–3220.
- Zabka, J., Ndiaye, I., Alcaraz, C., Romanzin, C., Polasek, M., 2014. Experimental and theoretical study of the mechanism of formation of astrochemically important $C_{2n+1}N^-$ anions via ion/molecule reactions. *International Journal of Mass Spectrometry* 367, 1–9.
- Zabka, J., Romanzin, C., Alcaraz, C., Polasek, M., 2012. Anion chemistry on Titan: A possible route to large N-bearing hydrocarbons. *Icarus* 219 (1), 161–167.